Spectrophotometric Investigation of the Complexation Mechanism of 3–(Trifluoromethyl) Acetophenone

S. Saravanan[1*], G. Kanagan[2], G. Satheeshkumar[3], S.Pari[4], R. Sambasivam[5]

[1,2,3,4]Department of Physics, National College (Autonomous), Triuchirappalli -620 001
[5]Department of Physics, Urumu Dhanalakshmi College, Triuchirappalli-620 019

Abstract- The experimental and theoretical study on the structures and vibrations of 3-TRIFLUOROMETHYL ACETOPHENONE (abbreviated as 3TFMAP) are presented. The FT-IR and FT-Raman spectra of the title compound have been recorded in the region $4000-400$ cm^{-1} and $3500-100$ cm^{-1} respectively. The molecular structures, vibrational wavenumbers, infrared intensities and Raman activities were calculated using DFT (B3LYP) method with 6-31+G (d) basis set. The most stable conformer of 3TFMAP is identified from the computational results. HOMO and LUMO energies were determined by time-dependent TD-DFT approach. Molecular electrostatic potential map also analysis by this present compound, respectively.

Keywords- TRIFLUOROMETHYL ACETOPHENONE, FT-IR,FT-Raman, HOMO and LUMO, Molecular electrostatic potential (MEP)

I. INTRODUCTION

Acetophenone is one of the most aromatic carbonyl, which shows interesting photochemical properties [1, 2]. Acetophenone are compound that exhibit interesting physicochemical and biological properties. They are found in nature [3, 4] and they can also be obtained by means of diverse synthesis procedures [5, 6]. Antibacterial activity can be mentioned among its biological properties. A recent study has linked the antibacterial activity of 20 acetophenone with their structural characteristics by using electronic and topological indices [7]. On the other hand, substituted acetophenone are employed as synthesis reagents of several organic reactions. A well known one is the condensation reaction in alkaline medium of acetophenones and benzaldehydes in the synthesis of flavonoids (chalcones, flavones and flavanones) [8, 9]. This work was based on combined solid phase infrared and Raman vibrational spectroscopy and gas phase theoretical calculation with the Density Functional Theory (DFT) method. DFT approaches, especially those using hybrid functional, have evolved to a powerful and very reliable tool and been routinely used for the determination of various molecular properties. B3LYP functional has been previously shown to provide an excellent compromise between accuracy and computational efficiency of vibrational spectra for large and medium size molecule [10−11]. Hence in this work, a systematic study on the optimized structure of the most stable conformer of the molecule, a detailed vibrational analysis based on FT-IR, FT-Raman inter and intra molecular charge transfer, Mulliken population analysis, and biological activity of the molecule based on its electrophilicity index have been carried out. The optimized geometry and vibrational wavenumbers are calculated only for the most stable conformer at DFT/B3LYP level of theory using 6-31+G (d) basis set. The conformers IV and V form are more stable than others. The vibrational wavenumber of the conformer IV of 3TFMAP have also been calculated. These calculations are valuable for providing an insight into the vibrational spectrum and molecular parameters. The stable position of 3TFMAP with respect to phenyl ring is obtained by performing the potential energy surface (PES) scan with B3LYP/6-31+G (d) level of theory.

II. EXPERIMENTAL DETAILS

The pure sample of 3TFMAP in the light yellow liquid form was purchased from the Lancaster Chemical Company (UK), with a stated purity of greater than 98% and it was used as such without further purification. The FT-IR spectrum of this compound was recorded in the region $4000-400$ cm^{-1} on IFS 66V spectrometer equipped with an MCT detector using KBr beam splitter and globar source. The FT-Raman spectrum of title molecule has been recorded using the 1064 nm line of a Nd:YAG laser as

excitation wavelength in the region 3500−100 cm^{-1} on a BRUKER model RFS 66V spectrometer. The reported wavenumbers are expected to the accurate within ±1 cm^{-1} resolution with 250 mW of power at the sample in both the techniques.

III. COMPUTATIONAL DETAILS

The gas phase geometry of the compound in the ground state was optimized by using DFT/B3LYP and LSDA levels with the standard basis set 6-31+G (d) on personal computer using GAUSSIAN 09W [12] program package, invoking gradient geometry optimization [13]. The global minimum energy conformer is used in the vibrational wavenumber calculation at the B3LYP and LSDA with using 6-31+G (d) level. Subsequently, the vibrational in association with the molecule were derived along with their IR intensity and Raman activity. In order to fit the theoretical wavenumbers to the experimental, the scaling factors have been introduced by using a least square optimization method. The HOMO−LUMO analysis has been carried out to explain the charge transfer within the molecule. The global hardness (η), global softness (σ), electronegativity (χ) and chemical potential (μ) have been calculated using the highest occupied molecular orbital (HOMO) and lowest unoccupied molecular orbital (LUMO). After the ground state geometry optimization, the excitation spectrum of the compound has been computed with at TD-DFT/6-31+G (d) level. Since solvent effects play an important role in absorption spectrum of the compound, in this paper, the time dependent self consistent field (TD-SCF) dealing with solvent effect was chosen in excitation energy calculations. The natural bonding orbital's (NBO) calculations [14] were performed using NBO 3.1 program as implemented in GAUSSIAN 09W package at DFT level in order to understand various second order interactions between the another subsystem, which is a measure of the intra molecular delocalization or hyper-conjugation. To check whether the chosen set of symmetric coordinates contribute maximum to the potential energy associated with the molecule, the PED has been carried out. The transformation of force field, subsequent normal coordinate analysis and calculation of the PED were done on a PC with the MOLVIB program (Version 7.0–G77) written by Sundius [15]. The complete information's regarding population of electrons in sub-shells of atomic orbital's and electron densities of an atom in the title molecule.

Prediction of Raman intensity

The Raman activities (S_i) calculated with the GAUSSIAN 09W Program were converted to Raman intensities (I_i) using the following relationship derived from the intensity theory of Raman scattering [16, 17].

$$I_i = \frac{f(\upsilon_0 - \upsilon_i)^4 S_i}{\upsilon_i[1 - \exp(-hc\upsilon_i/kT)]}$$

where υ_0 is the laser exciting frequency in cm^{-1} (in this work, we have used the excitation wavenumber υ_0=9398.5 cm^{-1}, which corresponds to the wavelength of 1064 nm of a Nd:YAG laser), υ_i is the vibrational wavenumber of the ith normal mode (in cm^{-1}) and S_i is the Raman scattering activity of the normal mode υ_i, f (is the constant equal to 10^{-12}) is a suitably chosen common normalization factor for all peak intensities. h, k, c, and T are Planck constant, Boltzmann constant, speed of light, and temperature in Kelvin, respectively.

IV. RESULTS AND DISCUSSION

Vibrational spectral analysis

The goal of the vibrational analysis is to find vibrational modes connected with specific molecular structure of calculated compound. Vibrational frequencies were calculated by using B3LYP method with 6-31+G (d) for the table molecule having 20 atoms with 54 normal modes. In this study, the full set of 69 standard internal coordinates (containing 15 redundancies) for 3TFMAP were given in Table 1. From these, a non-redundant set of local symmetry coordinates were constructed by suitable linear combinations of internal coordinates are summarized in Table 1. This method is also useful for determining the mixing of other modes. But mostly the maximum contribution is accepted as the significant mode. The observed FT-IR and FT-Raman bands with their relative intensities, calculated wavenumbers and assignments are given in Table 5. The experimental FT-IR and FT-Raman spectra with corresponding theoretically simulated FT-IR and FT-Raman spectra for 3TFMAP are shown in Figs 2 and 3, respectively, where the calculated infrared intensities and Raman intensities are plotted against the vibrational frequencies. In the spectra, the theoretically simulated spectra are more regular than the experimental ones because many vibrations presenting in condensed phase lead to strong perturbation of infrared and Raman intensities of many other modes. The RMS error of the observed and calculated frequencies (unscaled) of 3TFMAP is quite obvious since the frequencies are calculated on the basis of quantum mechanical force fields usually differ appreciably from observed frequencies. This is partly due to the neglect of anharmonicity and partly due to the approximate nature of the quantum mechanical methods. In order to reproduce the calculated frequencies, the scale factors were refined and optimized via a least squares refinement algorithm.

To calculate optimal scaling factors (λ), we employed as a least-square procedure using the below equation

$$\left[\lambda = \frac{\sum_{i}^{all} \omega_i^{theory} v_i^{expt}}{\sum_{i}^{all} \left(\omega_i^{theory} \right)^2} \right]$$ where ω_i^{theory} and v_i^{expt} are the ith theoretical harmonic and i^{th} experimental fundamental

frequencies (in cm^{-1}), respectively. The computed harmonic frequencies at B3LYP/6-31+G (d) level of basis set were scaled by 0.981 for frequencies lessthan 1700 cm^{-1} and 0.9615 for higher frequencies. These values are very close to the recommended scaling factor of 0.961 and 0.9968. The root mean square (RMS obtaine in

$$\left[RMS = \sqrt{\frac{1}{n-1} \sum_i^n \left(v_i^{cal} - v_i^{exp} \right)^2} \right]$$

The RMS error between un scaled B3LYP/6-31+G (d) and experimental frequencies are found to be 110 cm^{-1} and 102 cm^{-1} for FT-IR and FT-Raman, respectively.
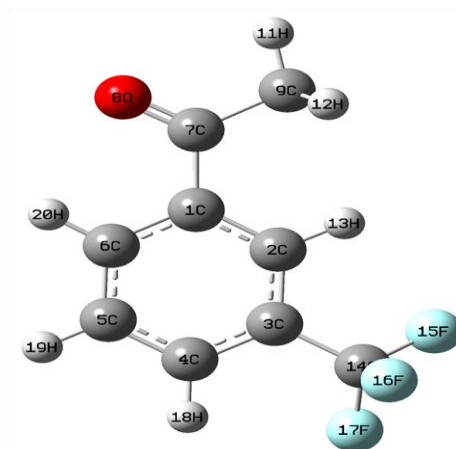

Fig. 1 The molecular structure of 3-trifluoromethyl acetophenone

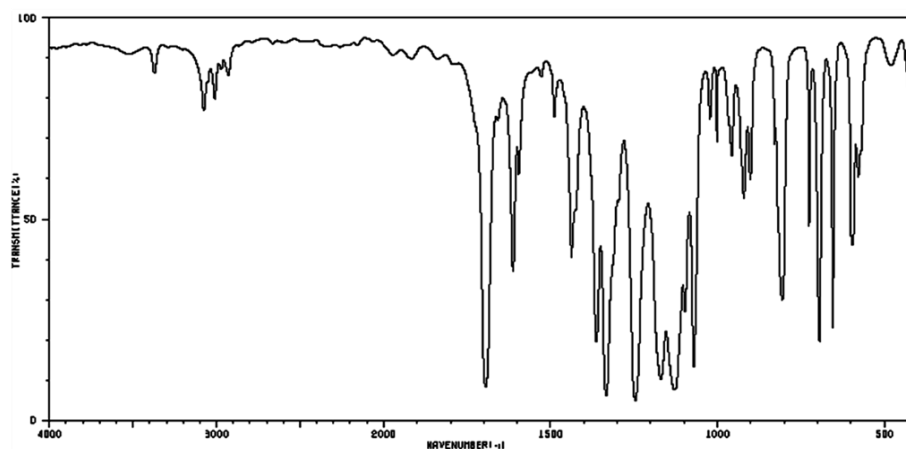
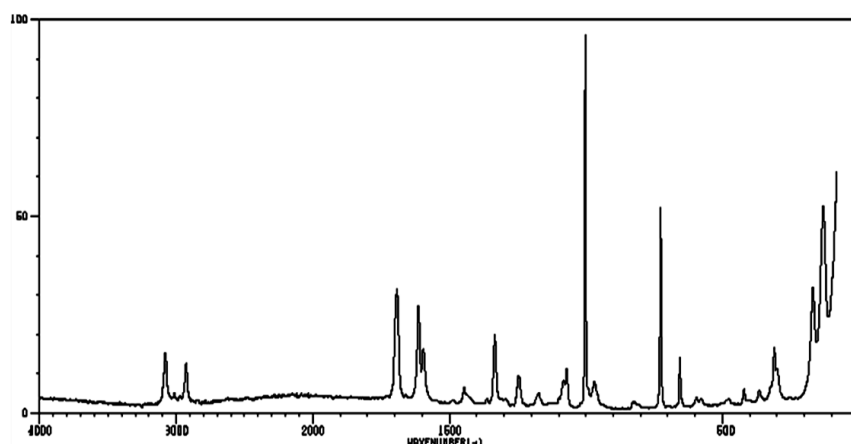Fig.2 The observed FT-IR spectra of 3-trifluoromethyl acetophenone

Fig..3 The observed FT-RAMAN spectra of 3-trifluoromethyl acetophenone

Table 1. Vibrational assignments of FT-IR and FT-Raman peaks long the theoretically computed wave numbers FT- IR intensity I_{IR} and Raman intensity I_{Rmn} and the percentage of potential energy distribution of 3-trifluromethyl accetophenone.

S.No	Observed wave number cm^{-1}		B3LYP/6-31+G (d)				assignments with % of PED^{C}
	FT-IR	FT-Raman	Calculated wavenumber cm^{-1}		I_{IR}	I_{Raman}	
			Unscaled	Scaled			
1			3231	3123	0.3	59.47	CH3asy
2		3073	3227	3082	6.12	142.28	CH3asy
3			3222	3073	0.88	80.48	CH3asy
4	3065		3201	3061	5.81	79.68	vCH
5			3165	3026	9.84	98.08	vCH
6	3000		3109	3002	6.98	42.78	vCH
7	2934	2926	3051	2931	2.8	133.5	vCH
8	1695	1682	1760	1690	200.5	66.02	vC=O
9	1608	1609	1658	1610	18.42	50.5	vCC
10	1586	1585	1637	1587	15.98	42.3	βCH
11	1532		1529	1533	4.04	1.43	vCC
12	1489		1502	1492	12.99	9.47	CH3sciss
13			1493	1472	10.58	6.77	vCC
14	1434	1439	1470	1435	25.26	1.84	CH3wag
15			1410	1362	49.09	2.62	βCH
16	1336		1372	1339	2.43	1.6	vCC
17		1329	1343	1327	125.61	15.03	βCH
18			1336	1312	87.97	24.56	βCH
19	1250	1256	1261	1254	335.28	11.1	CH3rock
20	1173	1182	1205	1178	6.67	5.66	vCC
21	1130		1170	1136	143.26	1.55	vCC
22			1126	1092	186.01	1.83	vCC

23			1120	1088	148.19	4.16	νCF
24	1086		1108	1083	10.8	6.03	νCF
25	1065	1073	1084	1067	109.87	12.23	βCH
26			1054	1042	0.67	0.35	νCC
27	1010		1017	1009	2.9	35.35	νCC
28	989	1000	1016	996	0.56	0.08	νCF
29		963	967	968	25.5	6.67	νCH
30	946		964	951	0.68	0.15	βCC
31	914		930	912	14.36	0.15	νCH
32		841	834	846	10.66	1.22	βCC
33	797		827	802	37.39	0.22	νCH
34	721		723	726	3.3	15.71	νCF
35	691		705	696	25.24	0.03	νCH
36		658	659	662	7.81	2.32	CF_3
37	648		659	651	10.02	0.9	CF_3
38	585	609	604	592	30.57	1.69	νCC
39	574	573	572	576	1.03	0.85	CF_3
40		487	567	493	3.78	0.42	CF_3
41			480	462	1.17	0.74	νCC
42			480	461	0.36	0.39	CF_{3ASSY}
43		414	427	414	0.09	0.15	νCF
44			392	390	2.36	1.84	CF_{3ASYS}
45		353	364	351	0.65	2.02	CF_{3SCISS}
46		304	326	301	0.18	0.77	CF_{3WAG}
47			305	296	2.4	4.98	νCC
48			243	229	2.64	0.1	CF_{3IPR}
49		158	164	157	0.21	0.61	νCC
50			164	156	0.02	1.65	CF_{3OPR}
51			128	121	4.09	0.3	CH3twist
52		85	90	84	0.13	3.07	CF_3
53			49	42	7.23	0.72	νCC
54			14	12	0.06	1.14	CF_{3TWIST}

ss – sym. Stretching, ss – sym. Stretching, ipb – in-plane-bending, opb – out-of-plane bending-, sb – sym.bending, ipr – in-plane rocking, opr – out-of-plane rocking, sciss – scissoring- rock – rocking-wag – wagging- twist – twisting. Assignments: ν - stretching-β - in-plane bending- γ- out-of-plane bending.

Phenyl ring modes:

The benzene ring possesses six stretching vibrations of which the four with the highest frequencies occurring near 1600, 1580, 1490 and 1440 cm^{-1} [18]. Generally, the C−C stretching vibrations in aromatic compounds give the bands in the region of 1650−1430 cm^{-1} [19]. In our title compound the prominent peaks at 1640, 1601, 1486, 1281 and 1258 in FT-IR and peaks at 1604, 1561, 1325, 1294 1262 and 1200 cm^{-1} in FT-Raman are due to C−C stretching vibrations. The theoretically computed values (mode no's 22−24, 27, 38, 41−45 and 47−50) are good agreement with experimental values. The frequency observed in FT-IR spectrum at 815 cm^{-1} have been assigned to ring breathing and corresponding vibration appear in FT-Raman spectrum at 812 cm^{-1} shows good agreement with experimental values. Usually an in-plane deformation is at higher frequencies than the out-of-plane deformations [20]. In the present molecule, the bands occurring at 1096, 1045, 685, 657, 623 and 476 cm^{-1} in FT-IR and in FT-Raman bands at 1056, 681 and 625 cm^{-1} are assigned to CCC in-plane bending modes. The CCC out-of-plane

bending modes of 3TFMAP is theoretically calculated at 316, 151, 144, 142, 132, 92, 71, 48, 42 and 19 in B3LYP method using 6-31+G (d) basis set, respectively.

C−H vibrations

The aromatic structure shows the presence of C−H stretching vibration in the region 3100−3000 cm^{-1}, which is the characteristic region for the ready identification of C−H stretching vibrations [21] Gunasekaran et al. [22] have reported the presence of C−H stretching vibrations in the region 3100−3000 cm^{-1} for asymmetric stretching vibrations and 2990−2850 cm^{-1} for symmetric stretching vibrations. In the present molecule, the FT-IR band at 3073 cm^{-1} and 3045 cm^{-1} in FT-Raman band are assigned to C−H asymmetric and symmetric stretching vibrations. Substitution sensitive C−H in-plane bending vibrations lie in the region 1300−1000 cm^{-1} [23, 24]. In 3TFMAP, very weak FT-IR band at 1157 cm^{-1} and FT-Raman band at 1169 cm^{-1} with very weak intensity are assigned to C−H in-plane bending vibrations. Bands involving the C−H out-of-plane bending vibrations appear in the range 1000−675 cm^{-1} [25]. The FT-IR bands observed at 988 and 804 cm^{-1} and FT-Raman bands at 950 and 781 cm^{-1} with weak intensity are assigned to C−H out-of-plane bending vibrations. They are good agreement with literature value [26].

Methyl vibrations

The title molecule 3TFMAP, under consideration possesses one CH$_3$ group in the para position of the ring along with C=O and hexyl group. Methyl groups are generally referred to an electron-donating substituent's in the aromatic ring system. For the assignments of CH$_3$ group frequencies on can expect nine fundamentals can be associated to each CH$_3$ group, namely the asymmetrical stretching (CH$_3$ass), symmetrical stretching (CH$_3$ss), in-plane bending (CH$_3$ipb), out-of-plane bending (CH$_3$opb), symmetric bending (CH$_3$sb), in-plane rocking (CH$_3$ipr), out-of-plane rocking (CH$_3$opr) and twisting (CH$_3$twist) modes. Whenever a methyl group is present in a compound, it gives rise to two asymmetric and one symmetric stretching is usually at higher wavenumber than the symmetric stretching. The asymmetric stretching vibrations of CH$_3$ are expected in the region 3000−2925 cm^{-1} and symmetric CH$_3$ stretching vibrations in the range 2940−2905 cm^{-1} [27, 28]. The observed asymmetric and symmetric stretching vibrations for CH$_3$ are at 3000 and 2966 cm^{-1} in FT-IR band and at 3000 and 2928 cm^{-1} in FT-Raman band. The calculated asymmetric and symmetric modes are 3004, 2998, 2976, 2969, 2930 and 2899 cm^{-1} at B3LYP methods are good agreement with observed data's. Two bending modes can occur within a methyl group. The first of these, the symmetric bending vibration, involves the in-phase of C−H bonds. The second the asymmetric bending vibrations, involves out-of-phase of the C−H bonds. The CH$_3$ in-plane bending vibrations are expected in the region 1485−1400 cm^{-1} [29]. The FT-IR band observed at 1486 cm^{-1} and the out-of-plane bending vibration coupled with CH$_3$ in-plane bending vibration occurred at 1410 cm^{-1} in FT-IR spectrum. The theoretically computed wavenumbers are 1487, 1480, 1466 and 1413 cm^{-1} in B3LYP method with 6-31+G (d) basis set are best correlated with the experimental values. The CH$_3$ symmetric bending mode observed at 1379 cm^{-1} in FT-IR value are good agreement with theoretical values (1396 and 1393 cm^{-1}). Methyl rocking modes are mass sensitive and variable in position due to the interaction with skeletal stretching modes. Generally, the in-plane and out-of-plane rocking modes observed in the region 1120−1050 cm^{-1} and 900−800 cm^{-1} [30, 31]. In the present molecule, the FT-Raman spectra shows the band at 1112 cm^{-1} assigned to in-plane rocking and 826 cm^{-1} in FT-IR spectra are assigned to CH$_3$ out-of-plane rocking mode. As CH$_3$ twisting mode is expected below 400 cm^{-1}, the theoretically computed values are at 236, 182, 234 cm^{-1} in B3LYP methods are assigned to mode, for, no spectral measurements were possible in the region due to instrumental limits. The C−CH$_3$ stretching vibration observed at 1006 cm^{-1} FT-Raman spectra and C−CH$_3$ in-plane and out-of-plane bending vibrations are observed at 573 and 257 cm^{-1} in FT-IR and FT-Raman spectrum, respectively.

C=O vibrations

Carbonyl group vibrations in ketones are the best characteristic bands in vibrational spectra, and for this reason, such bands have been the subject of extensive studies [32, 33]. The intensity of these bands can increase because of conjugation, therefore, leads to the intensification of the Raman lines as well as the increased infrared band intensities. The carbonyl stretching vibrations in ketones are expected in the region 1715−1680 cm^{-1}. In this case, a very strong band at 1674 cm^{-1} in FT-IR and strong band at 1671 cm^{-1} in FT-Raman spectra are assigned as C=O in-plane bending vibration is found at 724 and 726 cm^{-1} in FT-IR and FT-Raman values is well agreement with calculated values 728 and 724 cm^{-1} at B3LYP/6-31+G (d) methods. The out-of-plane bending vibration of 3TFMAP, theoretically calculated at 211 and 209 cm^{-1} is excellent agreement with the literature value [34].

Mulliken atomic charge

Mulliken atomic charge calculation has an important role in the application of quantum chemical calculation to molecular system because of atomic charges effect dipole moment, molecular polarizability, electron structure, acidity-basicity behavior and more lot of properties of molecular systems [35]. The charge distributions over the atoms suggest the formation of donor and acceptor pairs involving the charge transfer in the molecule. In present molecule, the charge distribution calculated on the

basis of Mulliken method using B3LYP and LSDA method 6-31+G (d) basis set listed in Table 2 . From the results, it is clear that the C_1 atom of 3TFMAP which is attached to the functional group (C=O) experience a higher positive magnitude which is obviously due to the presence of electronegative atom which withdrawn electrons from C atoms of the ring. In present case, C_7 atom is more acidic due to more positive`e charge in carbonyl group.

Table 2. Mulliken's population analysis of 3-trifluromethyl accetophenone at B3LYP/6-31+G (d) and HF/6-31+G (d) method Atom No.	MullikenAtomic charge	
	B3LYP 631+G(d)	HF 631+G (d)
C1	0.9232	0.8541
C2	-0.4315	-0.169
C3	-1.7726	-1.4076
C4	-0.266	-0.4831
C5	-0.3271	-0.3172
C6	0.3769	0.3159
C7	0.5082	0.136
O8	-0.424	-0.4223
C9	-0.8176	-0.7297
H10	0.2332	0.1975
H11	0.2463	0.2412
H12	0.2336	0.2437
H13	0.214	0.196
C14	1.5446	1.5639
F15	-0.3085	-0.2589
F16	-0.2693	-0.2599
F17	-0.3062	-0.3303
H18	0.2153	0.2121
H19	0.1976	0.1955
H20	0.2299	0.2219

Frontier molecular orbital's (FMOs)

The most important orbital's in molecule is the frontier molecular orbital's, called highest occupied molecular orbital (HOMO) and lowest unoccupied molecular orbital (LUMO). These orbitals determine the way of molecule interacts with other species. The frontier molecular energy gap helps to characterize the chemical reactivity and kinetic stability of the molecule. A molecule with a small frontier orbital gap is more polarizable and is generally associated with a high chemical reactivity, low kinetic stability and is also termed as soft molecule [35]. The low values of frontier orbital gap in IPDP it more chemical reactive and less kinetic stable. The frontier molecular orbital's plays an important role in the electric and optical properties [36]. The conjugated molecules are characterized by a small highest occupied molecular orbital – lowest unoccupied molecular orbital (HOMO – LUMO) separation, which is the result of a significant degree of intramolecular charge transfer from the end-capping electron acceptor groups through π – conjugated path [37]. The 3D plot of the frontier orbital's HOMO and LUMO of DCPI molecule is shown in Fig. 4. The positive phase is red and negative phase one is green (For interpretation of the reference to color in the text, the reader is referred to the web version of the article). Many organic molecules, conjugated π electrons are characterized by large values of molecular first hyperpolarizabilities, were analyzed by means of vibrational spectroscopy [38,39]. In most cases, even in the absence of inversion symmetry, the strongest band in the FT-Raman spectrum is weak in the FT-IR spectrum vice versa. But the intramolecular charge transfer from the donor-acceptor group in a single – double bond conjugated path can induce large variations of both the dipole moment and the polarizability, making FT-IR and FT-Raman activity strong at the same time. The analysis of wave function indicates that the electron absorption corresponds to the transition from the ground state to the excited state and is mainly described by one. An electron excitatio from the high occupied molecular orbital to the lowest unoccupied molecular orbital (HOMO – LUMO) Generally, the energy gap between

the HOMO and LUMO decreases, it is easier for the electrons of the HOMO to be excited. The higher energy of HOMO, the easier it is for HOMO to donate electrons whereas it is easier for LUMO to accept electrons when the energy of LUMO is low. The energy values of HOMO and LUMO levels are computed to be -0.20937 a.u. and -0.06573 a.u., respectively, and energy difference is -12,1888 a.u. in B3LYP/6-31+G (d). The energy values of HOMO and LUMO levels in B3LYP/6-311++G (d, p) is to be -0.20796 a.u. and -0.06420 a.u. and energy difference is 3.9119 a.u., respectively
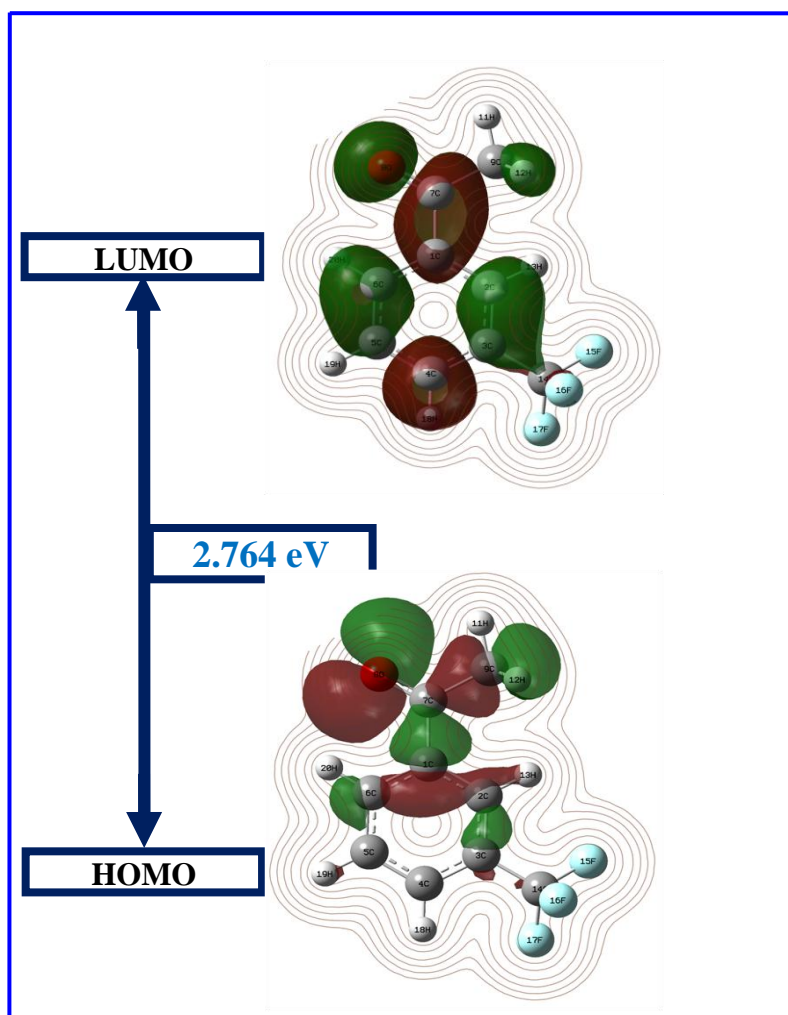

Fig. 4 The molecular orbitals and energies gap for the HOMO and LU of 3-trifluoromethyl acetophenone.

Molecular electrostatic potential (MEP)

Molecular electrostatic potential map sites for electrophilic attack and nucleophilic reactions as well as hydrogen bonding interactions [36−38]. A predict reactive sites for electrophilic attack for the title compound. MEP was calculated at the B3LYP/6-31+G (d) optimized geometry. For the systems studied the molecular electrostatic potential values were calculated as described using the equation:

$$V(r) = \sum \frac{Z_A}{|R_A - r|} - \int \frac{\rho(r')}{|r'-r|} dr$$

where the summation runs over all the nuclei A in the compound and polarization and reorganization effects are neglected. Z_A is the charge of the nucleus A, located at R_A and $\rho(r')$ is the electron density function of the molecule. The molecular electrostatic potential contour maps for positive and negative sites of the title molecule 4HAP are shown in Fig. 5. The MEP is a plot of electrostatic potential mapped onto the constant electron density surface. Different values of the electrostatic potential are represented by different colors. Red represents the regions of the most negative electrostatic potential and blue represent the regions of the most positive electrostatic potential. Potential increases in the order red < orange < yellow < green < blue. The color grading of resulting surface simultaneously displays molecular size, shape and electrostatic potential value which are very useful in research of molecular structure with its physiochemical property relationship [39]. As easily can be seen Fig.5, while region having the negative potential are over the electronegative atom (oxygen atom), the regions having the most positive potential are over the hydrogen atoms. As can be seen from the MEP of the title molecule, more reactive sites are near C=O group, the region having the most negative potential over the oxygen atom O_8, respectively.
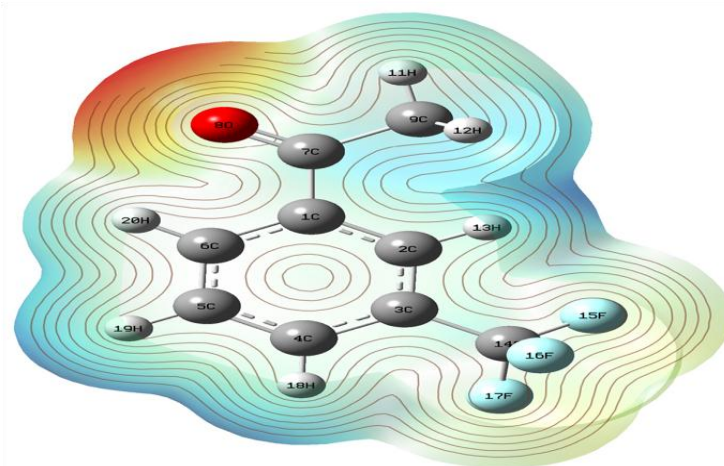

Fig.5   Molecular electrostatic potential map of 3-trifluoromethyl acetophenone

CONCLUSION

In the present work, the optimized molecular structure of the stable conformer, vibrational and electronic properties of the title compound have been calculated by DFT method (B3LYP) using 6-31+G (d) basis set. The optimized geometric parameters (bond lengths and bond angles) are theoretically determined and compared with the experimental results. Spectroscopic properties of the present molecule were examined by FT-IR and FT-Raman techniques. The complete vibrational assignments of wavenumbers are made on the basis of potential energy distribution (PED). The electronic properties are also calculated in different solvent with UV-Vis spectrum. The energies of MOs and the λ_{max} of the compound are also evaluated TD-DFT/B3LYP method with 6-31+G (d) basis set. The calculated HOMO, LUMO energy and frontier orbital energy gap values along with study for better understanding of charge transfer occur within the molecule.

REFERENCES

[1] R.N. Griffin, *Photochem. Photobiol.* 7, 1968, 159−173.
[2] L. Lindqvist, *J. Phys. Chem.* 76, 1972, 821−822.
[3] X. Zhang, L. Shan, H. Huang, X. Yang, X. Liang, A. Xing, H. Huang, X. Liu, J. Su, W. Zhang, *J. Pharm. Biomed. Anal.* 49, 2009, 715−725.

[4] Z.B. Liu, Y.S. Sun, J.H. Wang, H.F. Zhu, H.Y. Zhou, J.N. Hu, J. Wang, *Sep. Purif. Technol*. 64, 2008, 247–252.

[5] Y.R. Prasad, A.S. Rao, R. Rambabu, *Asian J. Chem*. 21, 2009, 907–914.

[6] S. Cacchi, G. Fabrizi, F. Gavazza, A. Goggiamani, *Org. Lett*. 5, 2003, 289–291.

[7] P.M. Sivakumar, G. Sheshayan, M. Doble, *Chem. Biol. Drug Des*. 72, 2008, 303–313.

[8] H.Z. Wei, L.C. Wing, H.L. Yuan, S.S. Yau, C.L. Yong, H.Y. Chi, *Heterocycles*, 45, 1997, 71–75.

[9] M.J. Climent, A. Corma, S. Iborra, A. Velty, *J. Catal*. 221, 2004, 474–482.

[10] H.G. Korth, M.I. de Heer, P. Mulder, *J. Phys. Chem*. 106, 2002, 8779–8789.

[11] A. Asensio, N. Kobko, J.J. Dannenberg, *J. Phys. Chem. A* 107, 2003, 6441–6443.

[12] M.J. Frisch, et al., GAUSSIAN 09, Revision A. 9, Gaussian, INC, Pittsburgh, 2009.

[13] H.B. Schlegel, *J. Comput. Chem*. 3, 1982, 214−218.

[14] E.D. Glendening, A.E. Reed, J.E. Carpenter, F. Weinhold. NBO Version 3.1.TCI. University of Wisconsin, Madison, 1998.

[15] T. Sundius, *J. Mol. Struct*. 218, 1990, 321−326; MOLVIB: A Program for Harmonic force field calculations. QCPE Program No. 807, 2002.

[16] P.L. Polavarapu, *J. Phys. Chem*. 94, 1990, 8106−8112.

[17] G. Keresztury, BT Raman spectroscopy. Theory, in: J.M. Chalmers, P.R. Griffiths (Eds.), Handbook of Vibrational Spectroscopy, Vol. 1, John Wiley & Sons Ltd., 2002, 71−87.

[18] Uwe Monkowius, Manfred Zabel, *Acta Cryst Sec. E* 64, 2008, m196.

[19] Min Zhang, Xian-You Yuan, Seik Weng Ng, *Acta Cryst. Sec. E* 66, 2010, o2917.

[20] E.G. Lewars, computational chemistry, Spriger Science, Business media. B.V., 2011, doi: 10:1007/978−90-481-3862-3-2.

[21] N.P.G. Roges, A Guide to the Complete Interpretation of Infrared Spectra of Organic Structures, Wiley, New York, 1994.

[22] V. Krishnakumar, N. Surumbakuzhali, S. Muthunatesan, *Spectrochim. Acta A* 71,2009, 1810–1813.

[23] G. Socrates, Infrared Characteristic Group Frequencies, John Wiley & Sons,Interscience Publication, New York, Brisbane, Toronto 1980

[24] G. Varsanyi, Assignments for Vibrational Spectra of Seven Hundred Benzene Derivatives, vol. 1/2, Academic Kiado, Budapset, 1973.

[25] S. Gunasekaran, R. ArunBalaji, S. Seshadri, S. Muthu, *Indian J. Pure Appl. Phys*. 46, 2008, 162–168.

[26] S.Saravanan, V. Balachandran, K. Viswanathan, *Spectrochim. Acta part A* 121, 2014, 685−697.

[27] V. Balachandran, K. Parimala, *J. Mol. Struct*. 1007, 2012, 136−145.

[28] V. Krishnakumar, V. Balachandran, *Spectrochim. Acta Part A* 63, 2006, 464−476.

[29] D. Sajan, J. Binoy, B. Pradeep, K. Venkatakrishnan, V. Kartha, I. Joe, V.Jayakumar, *Spectrochim. Acta Part A* 60, 2004, 173–180.

[30] S. Muthu, N.R. Sheela, S. Sampathkrishnan, *Mol. Simul*. 37, 2011, 1276−1288.

[31] K.B. Wiberg, A. Sharke, *Spectrochim. Acta A* 29, 1973, 583−594.

[32] M. Silverstein, G. Clayton Bassler, C. Morril, Spectroscopic identification of Organic Compounds, John Wiley, New York, 1981.

[33] N.B. Colthup, L.H. Daly, S.E. Wiberley, Introduction to Infrared and Raman Spectroscopy, Academic Press, New York, 1990.

[34] N. Roeges, A Guide to the Complete Interpretation of Infrared Spectra of Organic Structures, Wiley, New York, 1994.

[35] W.B. Tzeng, K. Narayanan, J.L. Lin, C.C. Tung, *Spectrochim. Acta Part A* 55, 1999, 153−162.

[36] A.M. Huralikoppi, Investigation on the Spectra of Some Substituted Aromatic Molecules; Ph.D thesis, Department of Physics, Karnataka University Dharrwad,1995.

[37] B. Smith, Infrared Spectral Interpretation, A Systematic Approach, CRC Press, Washington, DC, 1999.

[38] A.J. Abkowicz-Bienko, Z. Latajka, D.C. Bienko, D. Michalska, *Chem. Phys*. 250, 1999, 123−129.

[39] R.S. Mulliken, *J.Chem. Phys*. 2, 1934, 782−793.